DELIVERING BREAKTHROUGH SOLUTIONS

Uncertainty Quantification in Crater Formation for Gas-Granular Flows due to Plume Surface Interaction

NETL 2023 Workshop

Raymond Fontenot

Primarily Sourced from:
CFD Research Project: 10152
NASA Contract: 80NSSC21C0163

08/01/2023

Outline

- Motivation
- Sources of Uncertainty for PSI Simulations
- Modeling PSI
- Approaches to UQ
- Results

Motivation

Commentary from Apollo 12

- To me, it looked like a perfectly smooth, good area, between head crater and Surveyor crater and I started a vertical descent from a relatively high altitude, 300 feet at least . It may turn out that I actually backed up a little bit; but I don't think so. As soon as I got the vehicle stopped in horizontal **velocity at 300 feet, we picked up a tremendous amount of dust ; much more so than I expected**. I could see the boulders through the dust, but the **dust went as far as I could see in any direction and completely obliterated craters and anything else**. All I knew was there was ground underneath that dust. I had no problem with the dust, determining horizontal or lateral velocities, but **I couldn't tell what was underneath me**. I knew I was in a generally good area and I was just going to have to bite the bullet and land, because I couldn't tell whether there was a crater down there or not.
- At that point, the **dust was bad enough and I could obtain absolutely no attitude reference by looking at the horizon and the LM**. I had to use the 8-ball. I had attitude excursions in pitch of plus 10 and minus 10 , which happened while I was looking out the window making sure that the lateral and horizontal velocities were still nulled. I would allow the attitude of the vehicle to change by plus or minus 10 degrees in pitch and not be aware of it, and I had to go back in the cockpit and keep releveling the attitude of the vehicle on the 8-ball. I was on the gages in the cockpit doing that at the time the LUNAR CONTACT light came on. I had that much confidence in the gages. I was sure we were in a relatively smooth area. I had my head in the cockpit when the LUNAR CONTACT light came on and I instinctively hit the STOP button and that's how we got a shutoff in the air. **We were, I'd estimate, 2 or 3 feet in the air still when I shut down the engine and it dropped right on in**.
- I've already commented on the **blowing dust. I felt it was very bad**. It looked a lot worse to me than it did in the movies I saw of Neil 's landing. I'm going to have to wait and see our movies to determine if it doesn't show up as badly in the movies as it does to the eye. **Maybe we landed in an area that had more surface dust and we actually got more dust at landing**. It seemed to me that we got the dust much higher than Neil indicated. **It could be because we were in a hover, higher up coming down; I don't know. But we had dust from -- I think I called it around 300 feet.**
  - **Pete Conrad**
- After lunar liftoff **… a great quantity of dust floated free within the cabin**. This made breathing without a helmet difficult, and **enough particles were present in the cabin atmosphere to affect our vision**.
  - **Alan Bean**

Risks in Plume-Surface Interaction Induced Environments

EjectaSTORM Sensor flight test on a Masten Space Systems Lander sponsored by Flight Opportunity Program. Plume-surface interaction and ejecta cloud formation during propulsive landing.

Dust up on the Moon. Apollo 17 commander Eugene Cernan prepares to doff lunar dust-covered space suit. Credit: NASA

Figure 1. Mars InSight Lander post-landing surface cratering imagery (Credit: NASA/JPL).

Figure 2. Loci/GGFS Simulation of InSight Lander PSI-induced cratering (Credit: NASA/MSFC/ESSCA).

- Uncertainties in modeling of Plume-Surface Interaction frequently result in overly conservative designs of landing systems.
- High safety margins resulting in cost and performance penalties requires mandate of simulation capabilities to provide uncertainty characterization and quantification in predictions
- Where does the dust go (and what does it do) is also a major concern and unknown for future missions
- Key prediction capability for plume-surface interactions for landing operations is Loci/GGFS
  - Relies on models for gas-particle and particle-particle models with limited fidelity and considerable uncertainty in the applied range
  - Model complexity, immaturity, and sparsity of fundamentally physics-based models increases uncertainty in predictions
- Elevated urgency in needed sensitivity analysis capability

Sources of Uncertainty in PSI Simulations

The Plume-Surface Interaction (PSI) Environment

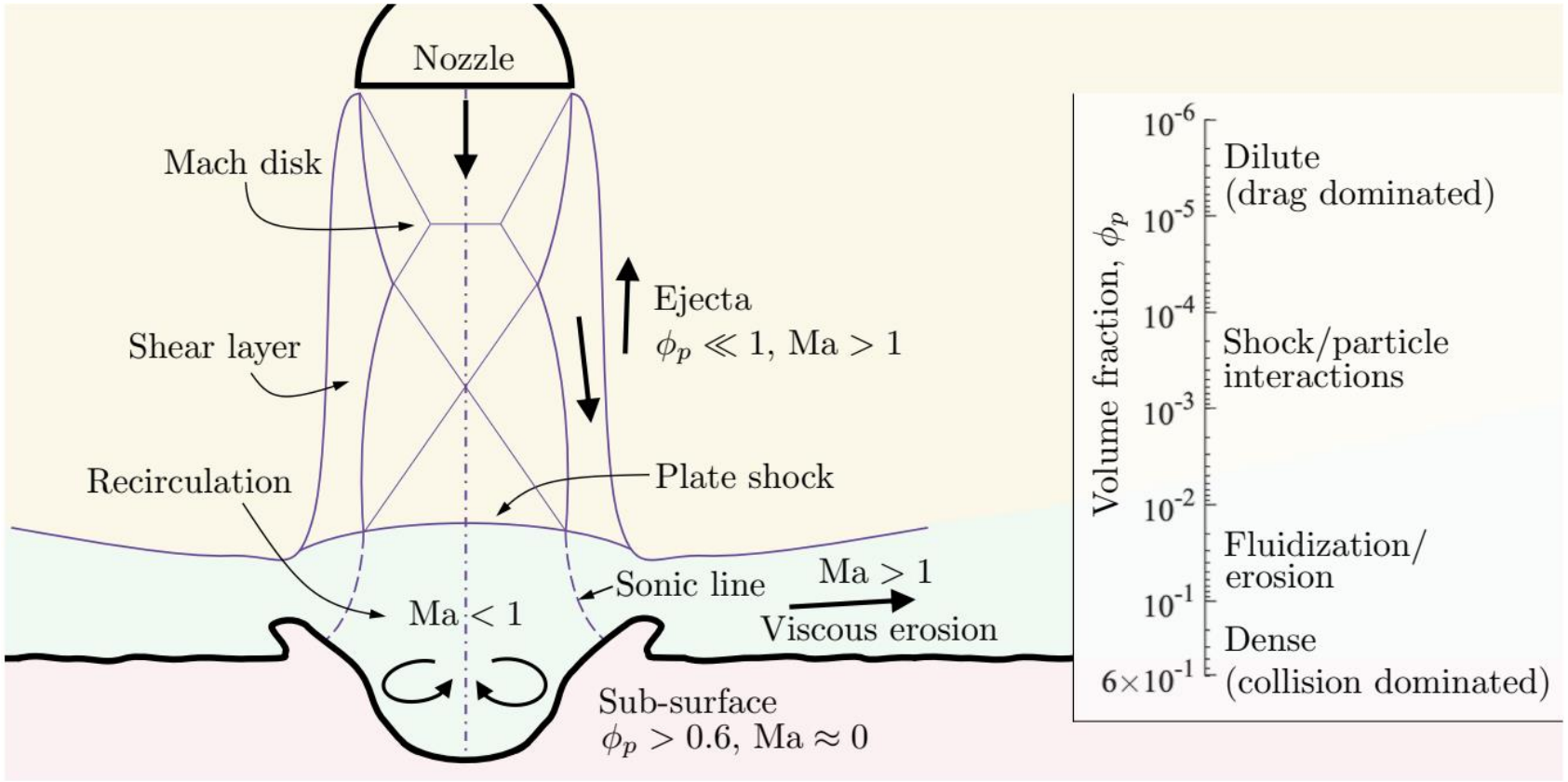

Figure 1. Schematic of the fluid-particle dynamics present during a landing event highlighting regions of varying Mach number, Ma, and volume fraction, α (ϕ_p) [1]

From The Ground Up: Lunar Regolith: Shapes and Sizes

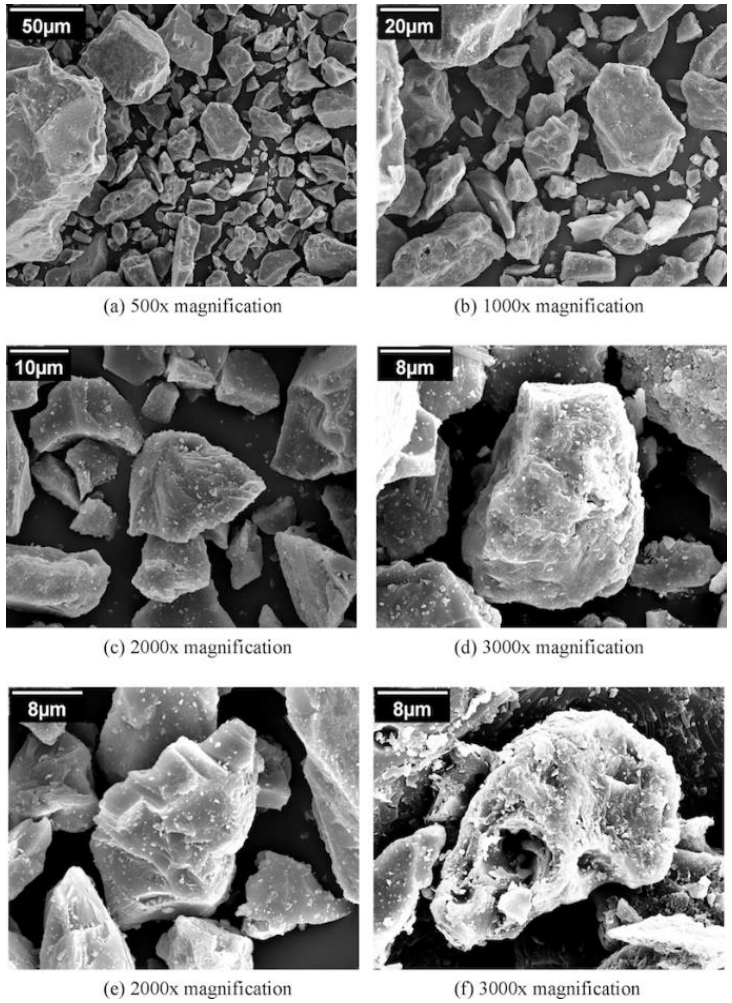

Figure. SEM images of JSC-1A particles at different magnification levels [2].

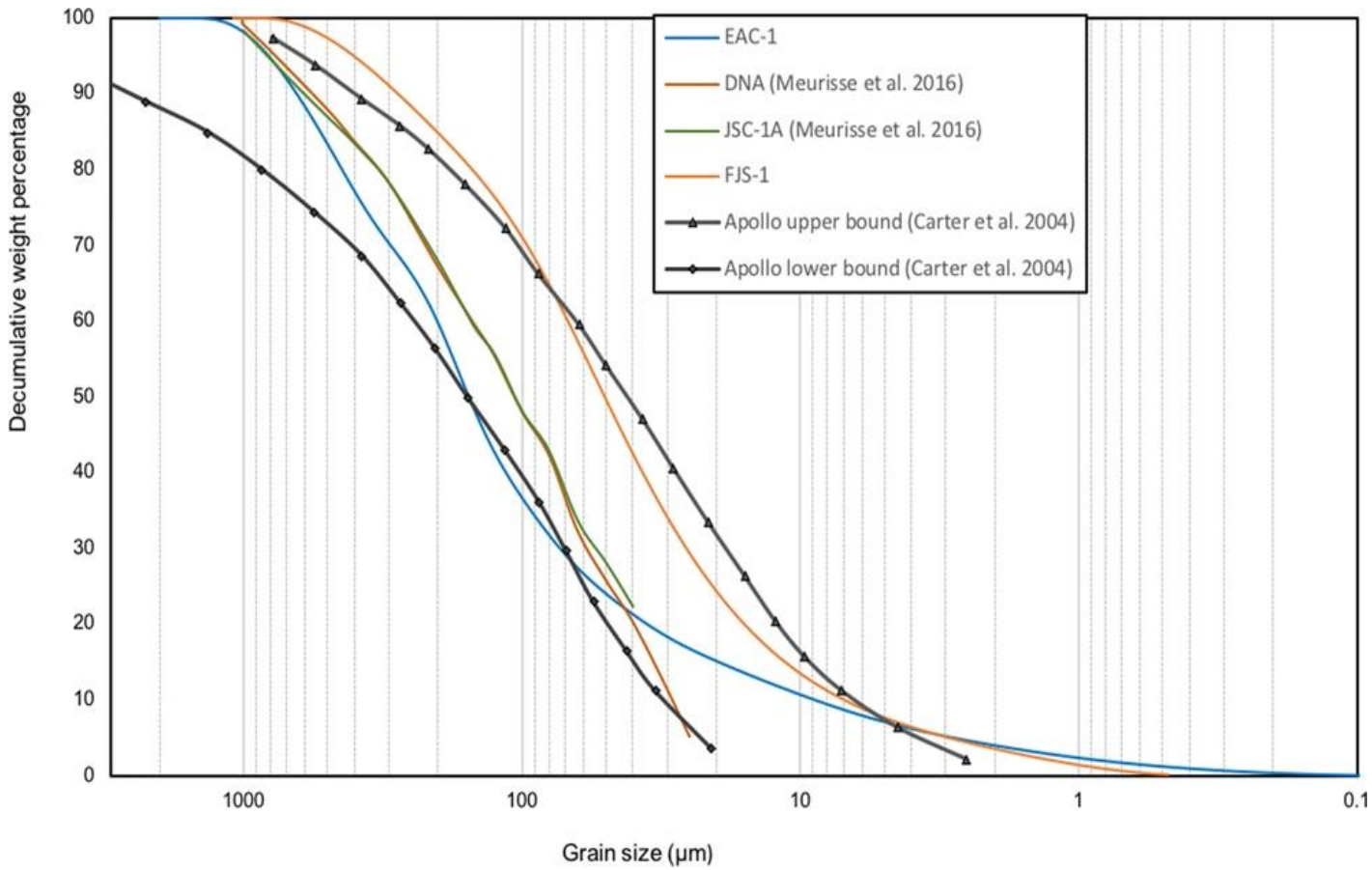

Figure. Grain size distribution curve. The grain size distribution of EAC-1A, DNA and JSC-1A, plotted together with the bulk grain size range of the Apollo samples from [3]

From The Ground Up: Lunar Regolith, It's a Sticky Business

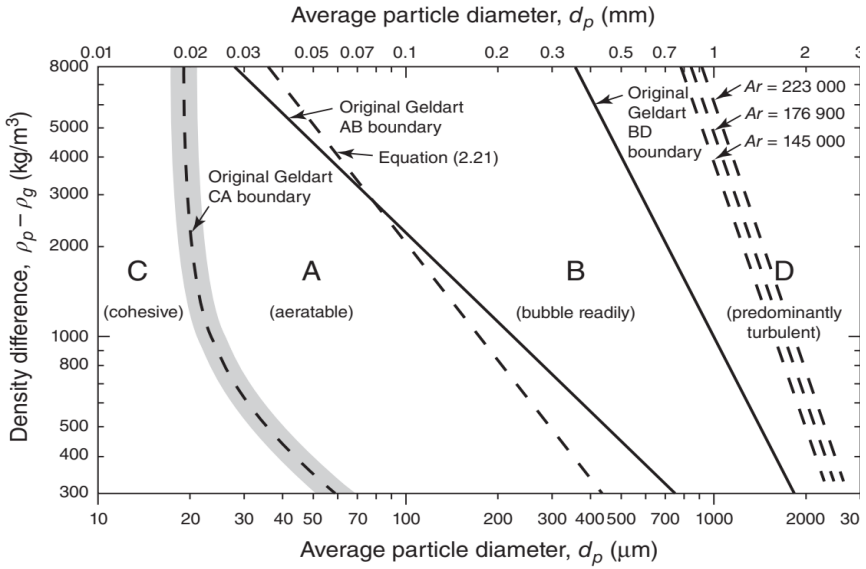

Geldart powder classification group boundaries for fluidization in air at 20°C and 1 atm pressure from [4]

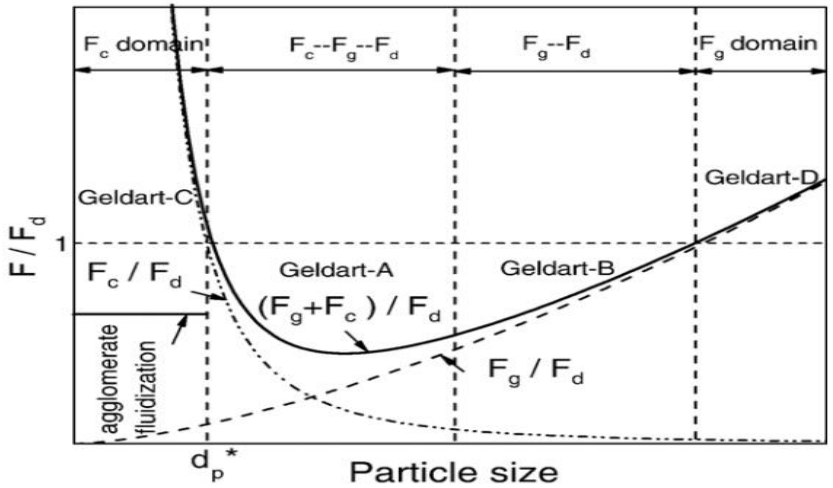

The relationship among gravity force, van der Waals force and drag force as a function of particle sizes and Geldart Classification from [5].

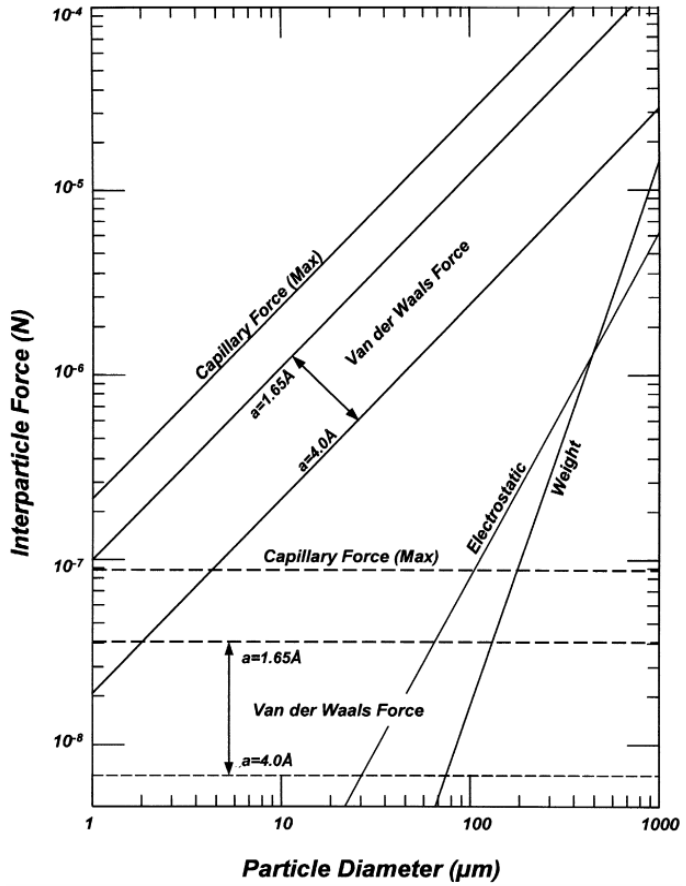

Interparticle Forces as a Function of Particle Diameter [6].

Geldart classifies particles as C, A, B, or D as a function of nominal/average particle diameter. **Also a function of temperature and gravity!**

- **Regolith falls into the C and A classification**
- Group C: Also known as Cohesive, these particles are dominated by interparticle cohesive forces that do not readily fluidize. Instead, these particles tend to form fissures through which gas flows. **(Less gravity, more cohesive!)**
- Group A: Also known as Aeratable, these particles are not dominated by interparticle forces, but they are non-negligible. They will readily fluidize if minimum fluidization velocity is reached.

Cohesive forces include: van der Waals, electrostatics **(don't forget the Lunar atmosphere is a cold plasma!),** capillary (**liquid and ice—very dependent on location**), and mechanical interlocking

From The Ground Up: Intergranular Challenges

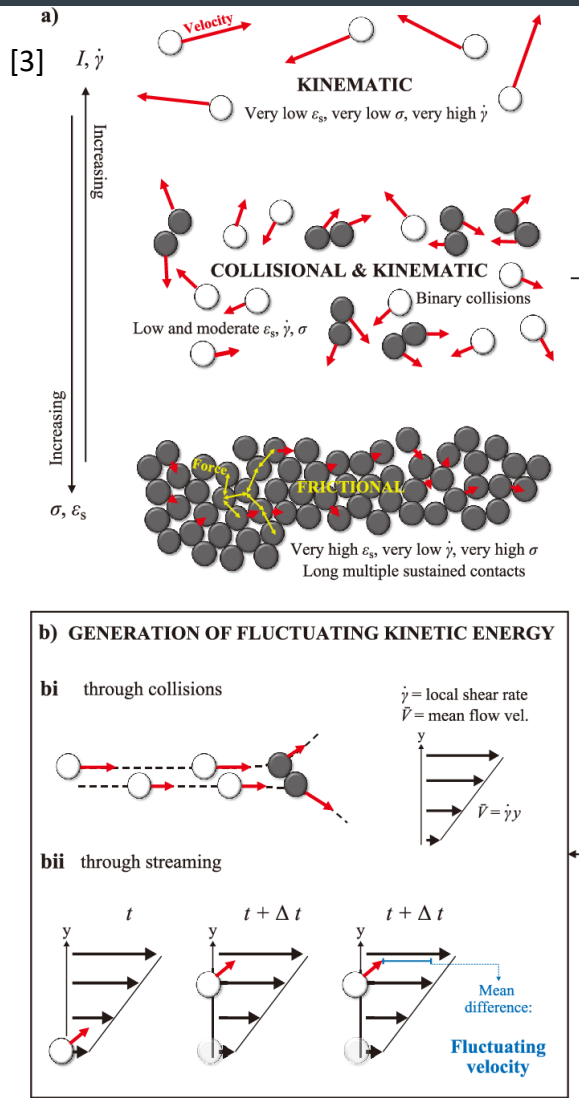

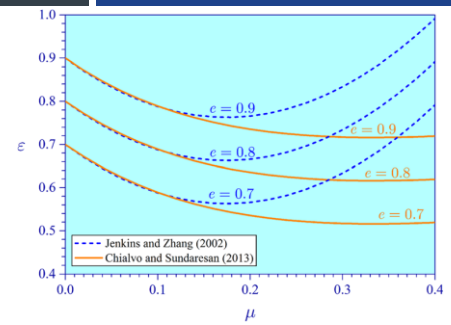

- Granular Frictional Stress [7]
  - $\sigma_s = \sigma_s^k + \sigma_s^c + \sigma_s^f$
  - Captures two extremes of granular flow: rapid shearing and quasi-static
  - Not founded on any proven physical basis [7,8]
  - No blending between regimes, but friction typically only allowed for $\alpha > 0.5$
- Coefficient of Restitution
  - Classifies type of collision: typically elastic vs. inelastic 0 < e < 1 (though e > 1 and e < 0 are admissible!)
  - $e = \frac{|\boldsymbol{v}_1 - \boldsymbol{v}_2|}{|\boldsymbol{u}_1 - \boldsymbol{u}_2|}$
  - Traditionally a fixed value associated with normal collisions (no variation between particle-particle or particle-wall)
    - Volume-averaging in methods is root-cause of this due to lack of discrete particle collisions
    - The coefficient of restitution should always be considered a paired property; that is the coefficient of restitution is inherently dependent on the material properties of each object and the kinematics of the collision (direction, angle of approach, etc.).
  - Recent models either a function of granular temperature or friction, but have wide variability (see figure, [9])
- Internal angle of friction
  - Measures steepest slope a granular material can take wrt a horizontal plane
  - Function of material density, surface area, surface morphology, particle sphericity, and gravity (due to change in cohesion) [10], and can be dynamic [11]!
  - Different values depending on how it is measured
  - Lunar regolith has known uncertainty 2°-10° [12]

Airborne! It's a Drag (and More)

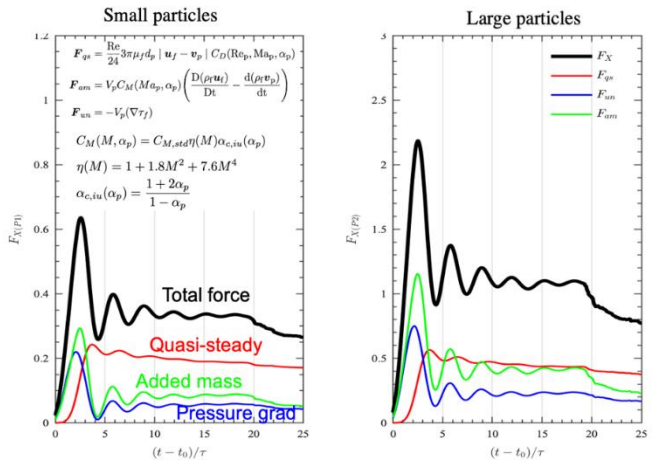

Individual contributions to the particle force during bidisperse shock-particle interaction [13]. Forces are the quasi-steady (drag)(F_{qs}), pressure grad (F_{un}), added-mass (F_{am}).

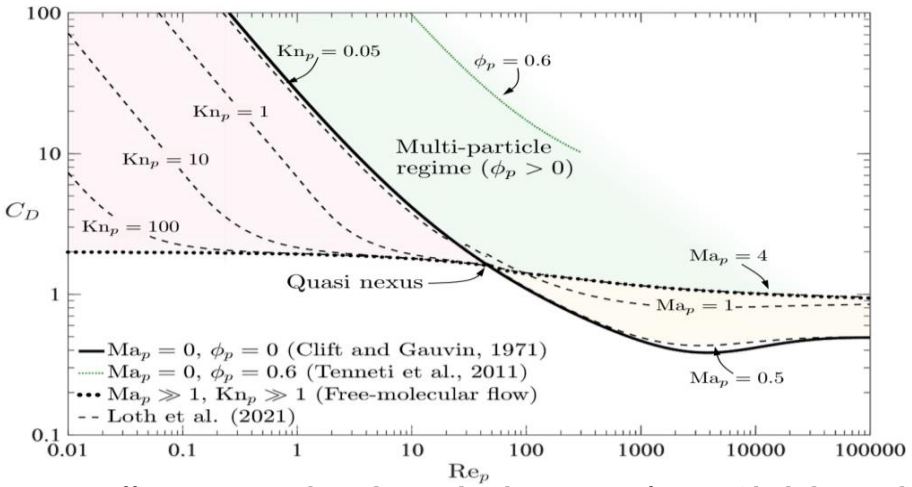

Drag coefficient on a spherical particle showing rarefaction (shaded in red) and compression (shaded in yellow) dominated regimes using the model proposed by Loth [14]. Multi-particle effects on the drag coefficient are shown in green. From [15]

- Interphase forces acting on particles include:
  - Drag
  - Lift (Magnus and Saffman/Shear)
  - Buoyancy
  - Time-History Forces: Added Mass and Viscous (Basset)
  - Pseudo Turbulent Kinetic Energy (PTKE)
  - Particle-Fluid-Particle (PFP)
  - Nanoscale forces (Brownian, Thermophoresis, etc)
- For multiparticle suspensions, the vast majority of models for the above forces in use were developed for incompressible flow
- Models for single particle drag have been developed and validated for both incompressible and compressible flow regimes
- Compressible flow models use a modification from the incompressible regime valid only for $\alpha<0.3$
- Models developed for compressible flow developed using narrow Re, α, M range due to complexity and expense of DNS
- With the exception of drag (and limited studies therein), little attention has been paid to rarified regime

Modeling PSI

How Do We Model PSI?

Increasing length scale

Particle-scale: *DNS*

- Direct solution to governing equations
- # particles: $O(10^2)$

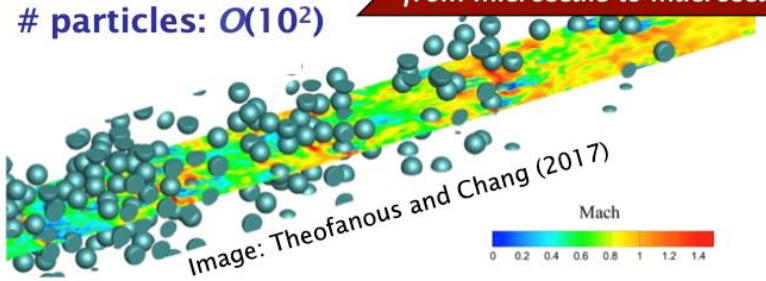

Physics can be lost when going directly from microscale to macroscale!

Intermediate scale: *Eulerian-Lagrangian*

- Description: Tracks individual particles and resolves collisions
- # particles: $O(10^8)$
- Requires models for gas-particle microphysics (e.g. drag)

Full-landing site: *Eulerian-based two-fluid model*

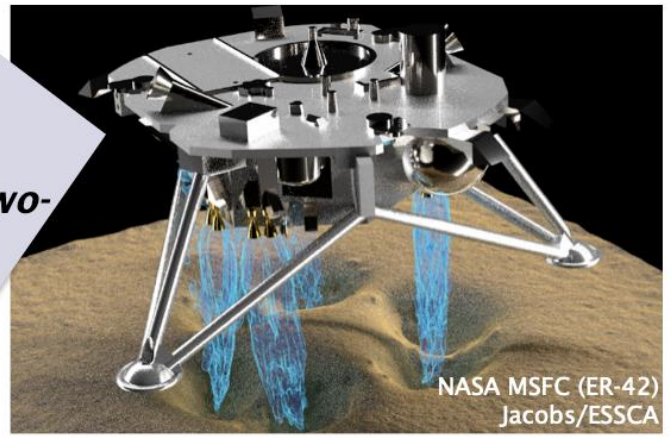

- Description: Treats gas and solid as a continuous fluid
- **# particles: cost *independent* of number of particles!**
- Relies heavily on constitutive models to account for important gas-particle and particle-particle interactions that **have not yet been developed or tested under relevant PSI conditions!**

- We can use higher-fidelity approaches to inform lower-order models
  - Comparison with canonical cases when experiments aren't enough
  - Sensitivity studies to extract models
- Practically speaking, the scale of the problem dictates we use an Eulerian approach for PSI

What Do You Mean Experiments Aren't Enough?

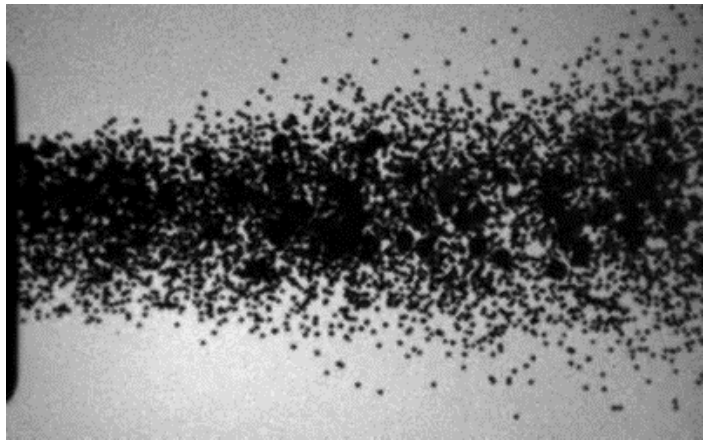

Gas-Granular Nozzle Experiments at a Heavy Particle Loading, from John Hopkins University as a part of NASA SBIR Phase II Project 9460

- There are a limited number of validation studies for PSI (LaMarche, Metzger, NASA's PFGT-1)
- Even for these limited conditions, the data is suspect at higher particle loading due to the near-impossibility to see anything
- It is worth noting there are experimental studies for gas-granular flows in the literature, but they are at much different flow conditions with limited extensibility into the PSI regime.
- Therefore, we are forced to turn to simulation-based approaches to extract any meaningful information—but isn't that a circular problem?

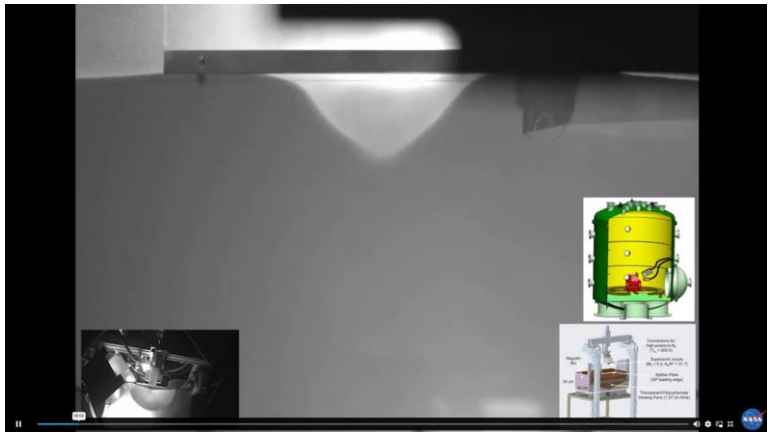

(Left) A 12-second vacuum chamber experiment with 150 micron single-size glass-sphere particle mixture, with a top-down image (inset bottom left) and models of the chamber and rig (inset bottom right), that was used for validation of the Gas-Granular Flow Solver, Loci/GGFS. The movie shows the crater formation viewed through the transparent viewing pane which is centered on the plume. The overhead view image shows the crater extent after test completion and settling of the crater wall material upon removal of the plume forces inside the crater. (Right) Validation (first 2 seconds) simulation performed with Loci/GGFS of experiment on shown on the left. *Jeff West, Manuel Gale, NASA/Marshall*

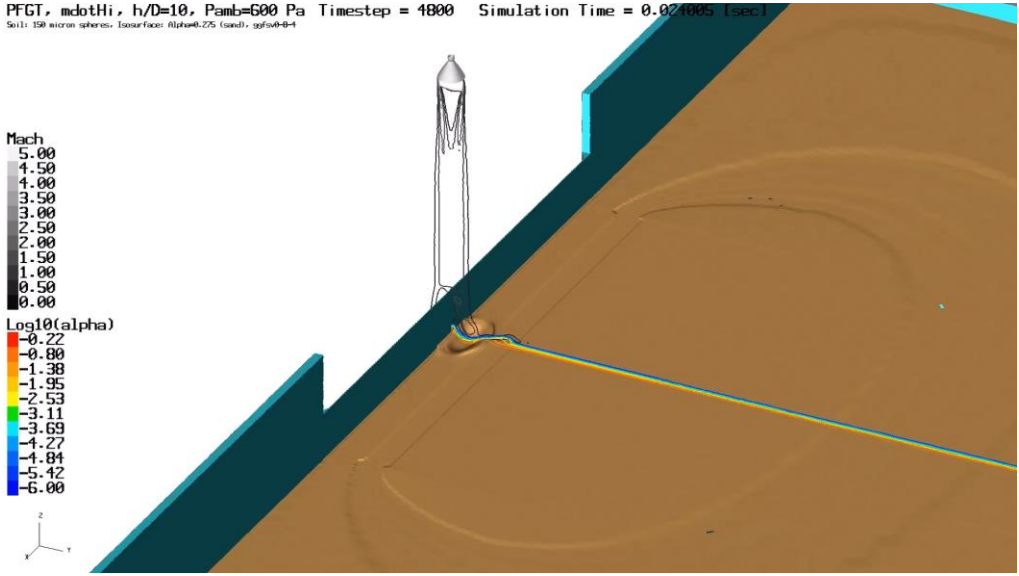

Gas-Granular Flow Solver (Loci/GGFS): Gas Equations

Key Features:

- EOS options include ideal gas, stiffened gas, Van der Waals, SRK, Peng-Robinson, tabular, elastic solid, Tait, JWL, HBMS.
- Realistic gas transport databases: transportDB and CHEMKIN.
- Turbulence: RANS and LES options.
- Pseudo-turbulent Reynolds stress.
- Operating Range:
  - Pressures: 0.01Pa to 10GPa+
  - Mach: incompressible to 10+
- Numerically verified using MMS.
- Validated for a wide variety of operating conditions.

Species:

$$\frac{\partial \alpha_g \rho_g Y_{g,k}}{\partial t} + \nabla \cdot \alpha_g \rho_g Y_{g,k} \vec{u}_g = \alpha_g \rho_g \nabla \cdot \vec{V}_{g,k}, \longrightarrow \mathbf{Y_{g,k}}$$

Continuity:

$$\frac{\partial \alpha_g \rho_g + \alpha_s \rho_s}{\partial t} + \nabla \cdot \left(\alpha_g \rho_g \vec{u}_g + \alpha_s \rho_s \vec{u}_s\right) = 0, \longrightarrow \mathbf{P_g}$$

Momentum:

$$\frac{\partial \alpha_g \rho_g \vec{u}_g}{\partial t} + \nabla \cdot \left[\alpha_g \left(\rho_g \vec{u}_g \otimes \vec{u}_g + p_g \bar{\bar{I}}\right)\right] = \nabla \cdot \left(\bar{\bar{\tau}}_g - \bar{\bar{\tau}}_{g,t}\right) - \nabla \cdot \left(\alpha_g \bar{\bar{R}}_u\right) + \alpha_g \rho_g \vec{g} + \left(p_g \bar{\bar{I}} - \frac{1}{\alpha_g} \bar{\bar{\tau}}_g\right) \nabla \alpha_g + F_{lift} + F_{drag} + F_{vm},$$

$$\longrightarrow \vec{u}_g$$

Energy:

$$\frac{\partial \alpha_g \rho_g e_{g,0}}{\partial t} + \nabla \cdot \left[\alpha_g \left(\rho_g e_{g,0} + p_g\right) \vec{u}_g\right] = \nabla \cdot \left[\vec{u}_g \cdot \left(\bar{\bar{\tau}}_g - \bar{\bar{\tau}}_{g,t}\right)\right] - \nabla \cdot \left(\alpha_g \vec{u}_g \cdot \bar{\bar{R}}_u\right) + I_{t_{g,s}} + \alpha_g \rho_g \vec{g} \cdot \vec{u}_g + \left(p_g \bar{\bar{I}} - \frac{1}{\alpha_g} \bar{\bar{\tau}}_g\right) \nabla \alpha_g \cdot \vec{u}_g + \nabla \cdot \vec{q}_g + \sum^{Ng} \nabla \cdot (\rho h V)_{g,i} + \left(F_{lift} + F_{drag} + F_{vm}\right) \cdot \vec{u}_g, \longrightarrow \mathbf{T_g}$$

Gas-Granular Flow Solver (Loci/GGFS): Granular Equations

Key Features:

- State-of-the-art polydisperse model for spherical and irregular shape particles (Garzo-Hrenya-Dufty and DEM-Derived Models).
- Discrete element method (DEM)-based shape effects.
- Particle-particle contact heat transfer.
- Internal energy + kinetic energy conservation.
- Drag, lift, convective-heat transfer between gas and solid have particle shape dependency.
- Fully hyperbolic form.
- Numerically verified using MMS.
- Validated for a wide variety of operating conditions.

Species:

$$\frac{\partial \alpha_s \rho_s Y_{s,k}}{\partial t} + \nabla \cdot \alpha_s \rho_s Y_{s,k} \vec{u}_s = -\nabla \cdot \vec{j_{s,k}}, \longrightarrow Y_{s,k}$$

Continuity:

$$\frac{\partial \alpha_s \rho_s}{\partial t} + \nabla \cdot \left(\alpha_s \rho_s \vec{u}_s\right) = 0, \longrightarrow \alpha_s$$

Momentum:

$$\frac{\partial \alpha_s \rho_s \vec{u}_s}{\partial t} + \nabla \cdot \left[\alpha_s \left(\rho_s \vec{u}_s \otimes \vec{u}_s + p_g \bar{\bar{I}}\right) + p_s \bar{\bar{I}}\right] = \nabla \cdot \left(\bar{\bar{\tau}}_s + \frac{\alpha_s}{\alpha_g} \bar{\bar{\tau}}_g\right) + \alpha_s \rho_s \vec{g} + \left(p_g \bar{\bar{I}} - \frac{1}{\alpha_g} \bar{\bar{\tau}}_g\right) \nabla \alpha_s - F_{lift} - F_{drag} - F_{vm}, \longrightarrow \vec{u}_s$$

Energy:

$$\frac{\partial \alpha_s \rho_s e_{s,0}}{\partial t} + \nabla \cdot \left[\left(\alpha_s \left(\rho_s e_{s,0} + p_g\right) + p_s\right) \vec{u}_s\right] = \nabla \cdot \left[\vec{u}_s \cdot \left(\bar{\bar{\tau}}_s + \frac{\alpha_s}{\alpha_g} \bar{\bar{\tau}}_g\right)\right] + \alpha_s \rho_s \vec{g} \cdot \vec{u}_s + \left(p_g \bar{\bar{I}} - \frac{1}{\alpha_g} \bar{\bar{\tau}}_g\right) \nabla \alpha_s \cdot \vec{u}_s + \sum_{i=1}^{Ns} \nabla \cdot (\rho h V)_{s,i} - (F_{lift} + F_{drag} + F_{vm}) \cdot \vec{u}_s + \nabla \cdot \vec{q}_s - I_{t_{g,s}}, \longrightarrow T_s$$

Granular Temperature:

$$\frac{3}{2}\left[\frac{\partial}{\partial t}\left(\alpha_s \rho_s Q\right) + \nabla \cdot \left(\alpha_s \rho_s Q \vec{u}\right)\right] = -\nabla \cdot \vec{q_T} - \nabla \cdot \left(\bar{\bar{P}} \cdot \vec{u}\right) - \frac{3}{2}\alpha_s \rho_s Q \zeta + \frac{3}{2} m_w Q \sum_{i=1}^{NS} \frac{1}{m_i} \nabla \cdot \vec{j_i} + \sum_{i=1}^{NS} \frac{\vec{F_i} \cdot \vec{j_i}}{m_i}, \longrightarrow Q$$

Approaches to UQ

Studying Model Sensitivities: An Overview

- There are two general approaches to sensitivity studies:
  - Non-intrusive: external methods which drive simulations based on analysis criteria for either
    - Uncertainty analysis: ensures efficient propagation of uncertainty in model inputs vs outputs
      - Monte Carlo (Sampling Methods)
      - Stochastic expansion
      - Surrogates
    - Sensitivity analysis: qualitative approaches to evaluate impact of uncertainty in model inputs vs outputs
      - Screening approaches, such as Morris One-at-A-Time (MOAT) or One-at-a-Time methods
      - Global Sensitivity Analysis, such as Variance-based (Sobol')
      - Entropy-based and moment-independent methods
  - Intrusive: require code modifications as sensitivities are derived from the actual numerical methods and models used
    - Forward/Backward Automatic Differentiation
    - Adjoint Methods

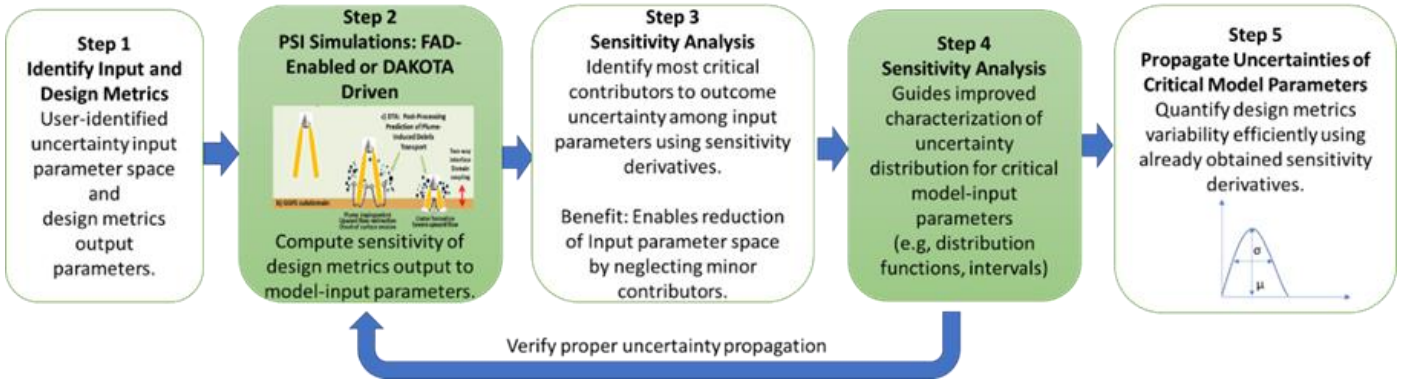

Non-Intrusive Uncertainty Quantification with SQUAT

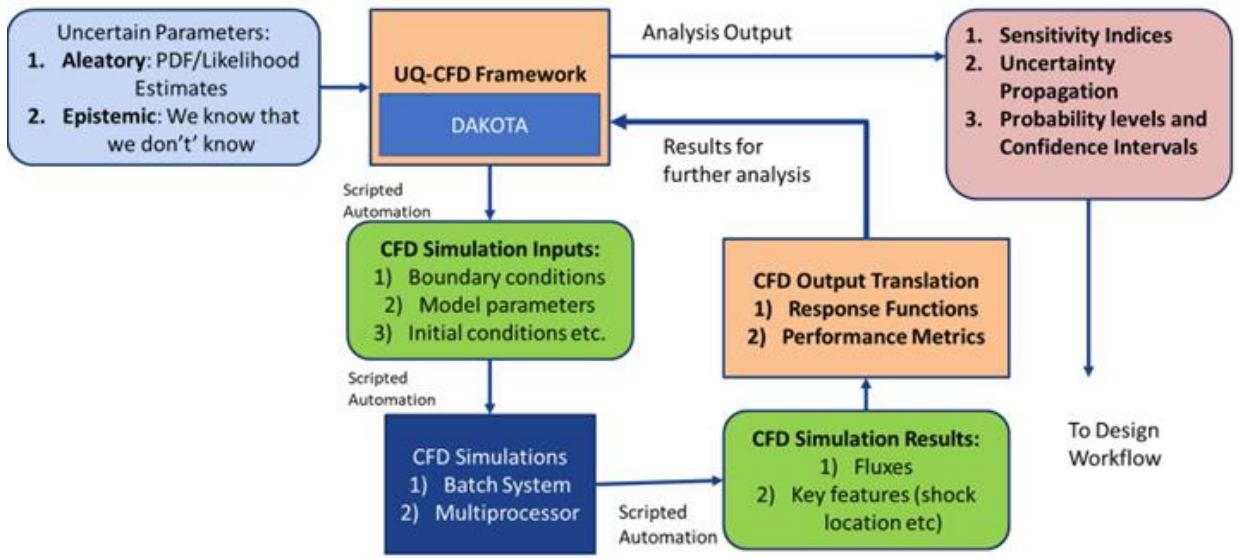

Sensitivity Quantification for Uncertainty Analysis Toolkit

- Non-intrusive methodology initially developed under NASA SBIR contract (Contract: NNX17CL48P)
  - Leverages DAKOTA, a state-of-the-art, robust, user friendly software from Sandia National Laboratories for optimization and UQ (GPL v2 license).
  - Fully featured including sensitivity analysis, parameter estimation, multi-constrained optimization etc. with a single interface (developed and deployed on NAS-PFE for 80NSSC20C0243).
  - Multiple simulations can be run in parallel and asynchronously.
  - Can build PDF and CDF of the system responses.
  - Two approaches to be used herein for sensitivity analysis
    - Morris One-At-A-Time (MOAT)
    - Sobol Indices (not shown herein)
- Used as verification and comparison for FAD—intrusive approach

Morris-One-at-a-Time

MOAT Basics:
- Global, derivative-based sensitivity method
- Input parameters are randomly varied to get an even spread across all inputs and do not overlap for any two cases.
- Test cases can be run in succession or simultaneously.
- Results produce the elementary effects of the input space on the output space under investigation.
- Can distinguish nonlinear coupling effects, but accuracy is highly dependent on step-size

d_i = elementary effects over the input space
r = the number of samples generated from this distribution
σ_i = the standard deviation of the input space
μ_i^* = the modified mean of the input space

$$d_i(\boldsymbol{x}) = \frac{y(\boldsymbol{x} + \Delta \boldsymbol{e}_i) - y(\boldsymbol{x})}{\Delta}$$

$$\mu_i^* = \frac{1}{r}\sum_{j=1}^{r}\left|d_i^{(j)}\right|$$

$$\sigma_i = \sqrt{\frac{1}{r}\sum_{j=1}^{r}(d_i^{(j)} - \mu_i)^2}$$

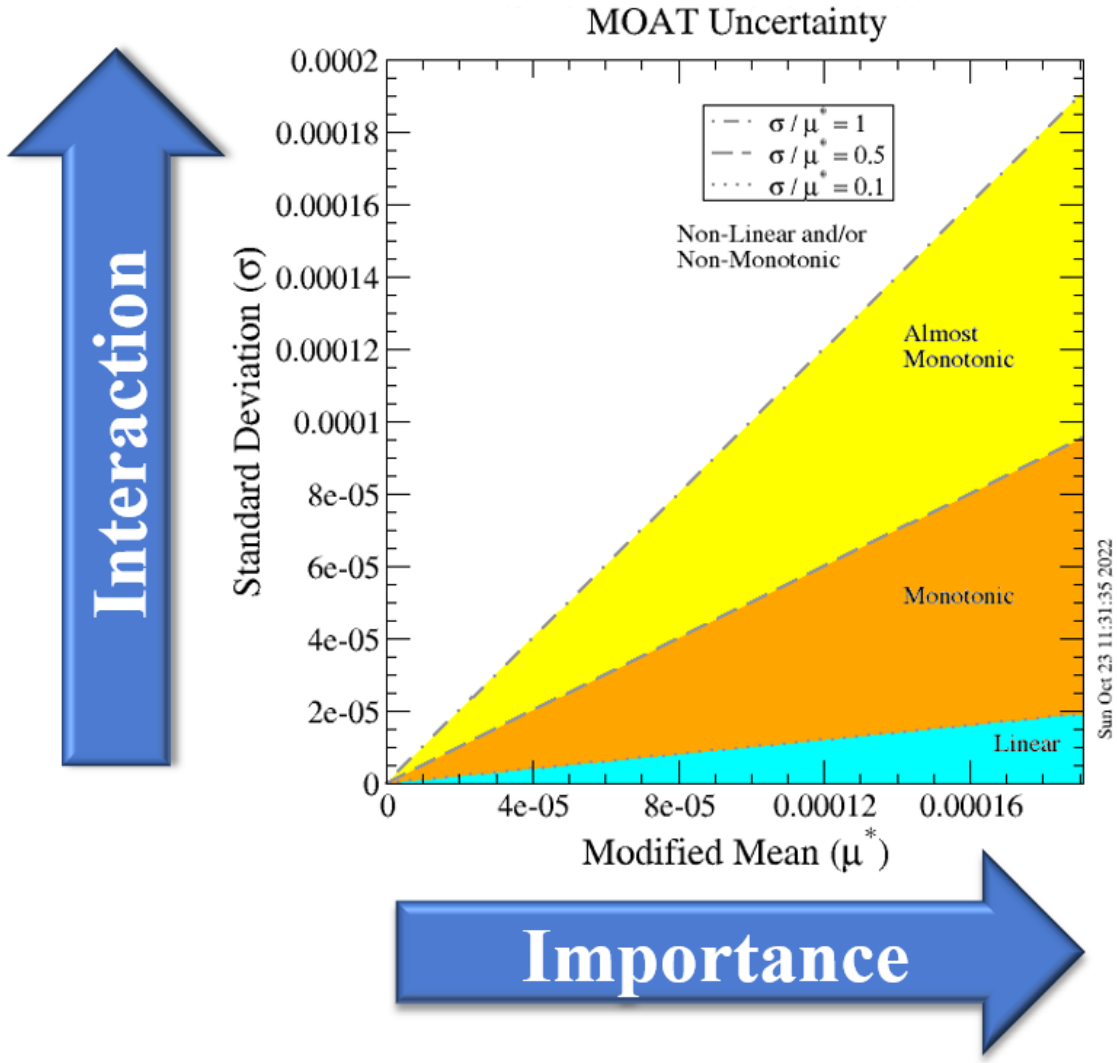

Forward Automatic Differentiation

- Forward automatic differentiation (FAD) is a mathematical method of sensitivity analysis.
- FAD computes sensitivity derivatives which can be normalized about nominal values to determine local sensitivity coefficients S_i

$$S_i = \frac{\boldsymbol{D_{0,i}}}{\boldsymbol{f_0}} \frac{\partial \boldsymbol{f}}{\partial \boldsymbol{D_i}} \quad (1)$$

  for a given model input parameters D with respect to an output f, with (f_0, D_0) representing the nominal values, and the sensitivity derivative.
- Local sensitivity coefficients can then be used to rank the effects of model input parameters to determine which are the most significant contributors to the uncertainty.
- Those model input parameters with the highest uncertainties can then be propagated to realize their effects on the simulation.

$$f(\mathbf{D}) = \mathrm{f}(\mathbf{D_0}) + \sum_{\mathbf{i=1}}^{\mathbf{n}} \frac{\partial \mathrm{f}}{\partial \mathbf{D_i}} \left(\mathbf{D_{0,i}} - \mathbf{D_i}\right) \quad (2)$$

- FAD facilitated in Loci codes with use of operator overloading such that 'normal' mode is not affected, and 'FAD' mode is enabled by compiler keywording and (^,^^) in the input deck
- Current Loci implementation of FAD can handle multiple inputs and one output at a time—so 1 simulation per output, and the cost per simulation grows approximately linearly with additional inputs.

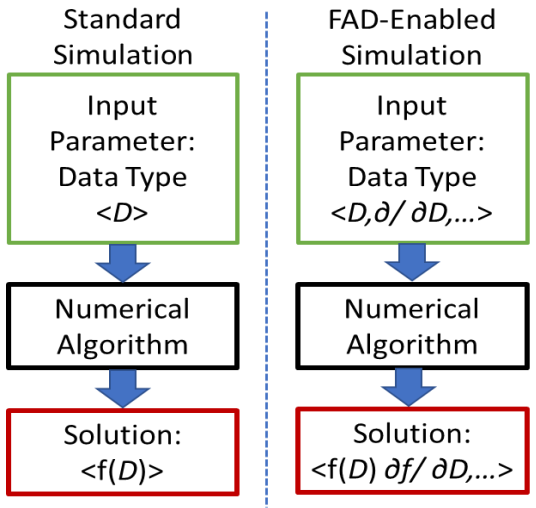

Comparison of the simulation proess using a standard data type and an FAD-enabled data type (dual number) in Loci.

Key Points:
- FAD easily implemented.
- Significantly fewer simulations compared to non-intrusive methods.

Results

Sensitivity Analysis on Relevant PSI Configuration

LaMarche Plume Surface Interaction:

- Jet impingement case into granular bed of monodisperse spherical steel balls
- Jet is 0.7747 cm in diameter placed 5 cm above bed
- Axisymmetric Simulation
- No turbulence in this analysis
- 200k iterations at dt=7.5e-6 s, ~1.5 s

Shape (D [mm] x L [mm])	Initial Solid Fraction	Solid Density [kg/m^3]	Coeff. Friction	Coeff. Rest.	$\alpha_{s_{min}}$
Sphere 1mm	0.63	7600	0.42	0.63	0.5

- Input sensitivities on jet mass inflow, internal angle of friction, particle diameter, and (FAD only) jet inflow temperature
  - Non-Intrusive: ±15 % variation
  - FAD: ±10% variation
- Output quantities of interest
  - Crater Depth
  - Crater Width
  - Mass Evacuated from Crater

fixedMass flow:
$\dot{m}_{gas} \approx 0.0024\ kg/s$

Regolith Depth:
$H = .12\ m$

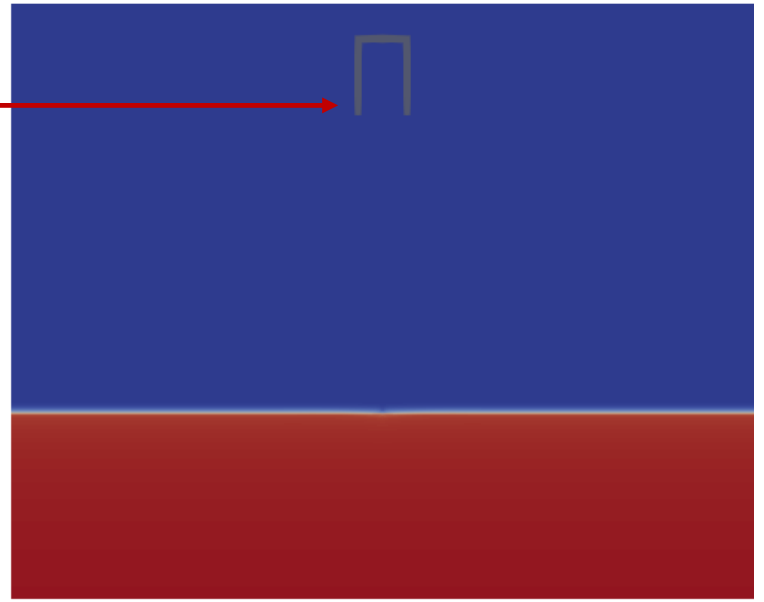

How Expensive is an Analysis?

Method	# of Runs	# of Nodes	CPUs per Node	Total CPUs	Total Runtime [hr]	Core-Hours
MOAT	32	40	20	800	457.6	365,864
Sobol	113+	29	28	812	TBD	TBD
Non-FAD	5	29	28	812	71.5	58,058
FAD (plot_freq = 100)	4	58	28	1624	236.0 (59 per run)	383,212
FAD (est. plot_freq = 1000)					198.2 (49.5 per run)	321,941

Key Points and Notes:

- Sobol analysis still on-going
- FAD/Non-FAD runs were run the same total length of time as other analysis (200k iterations) but as crater reached the bottom of domain ~35 k iterations and simulations are slightly different, direct comparison of timings is marginal
- FAD runs were set to output (unfortunately) every 100 iterations, so more comparable timing is estimated
- Costs for FAD still much cheaper (and fewer runs) than non-intrusive analysis

Demonstration on Relevant PSI Configuration: MOAT

LaMarche - MOAT Analysis

Mass Flux of Particulates @ Initial Bed Height

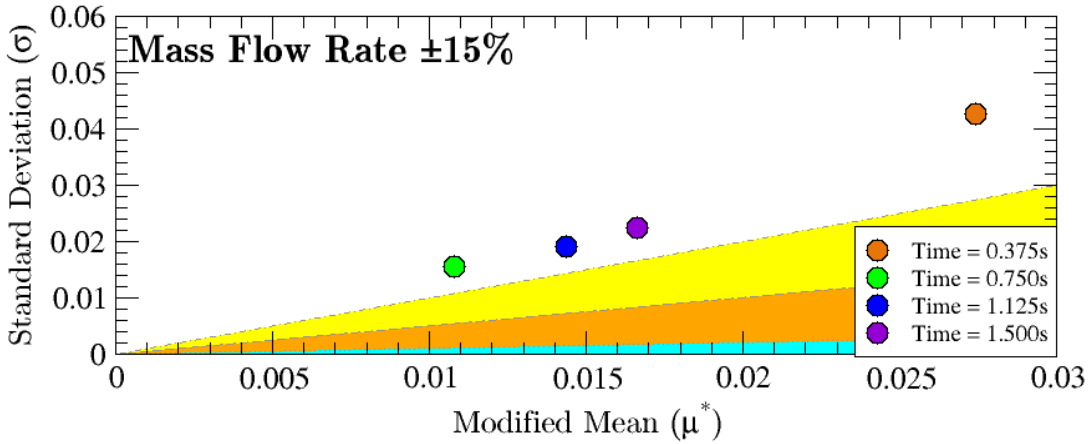

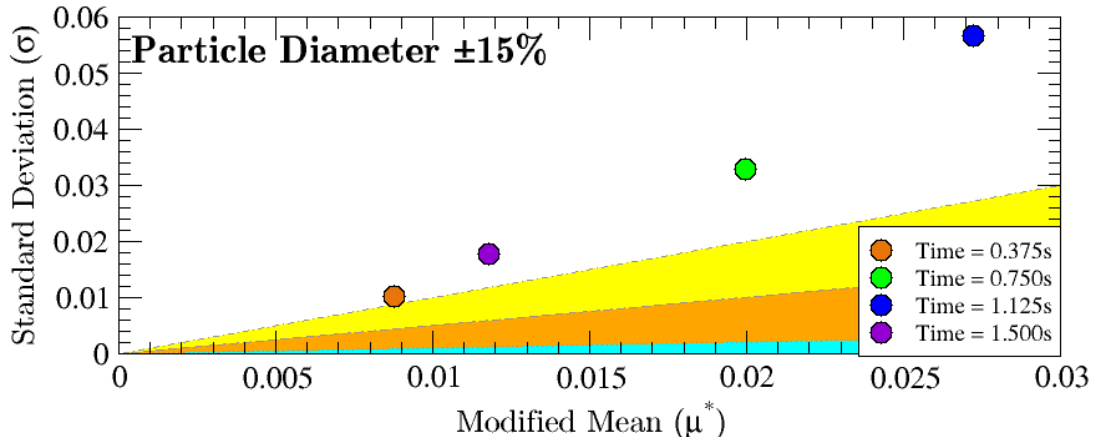

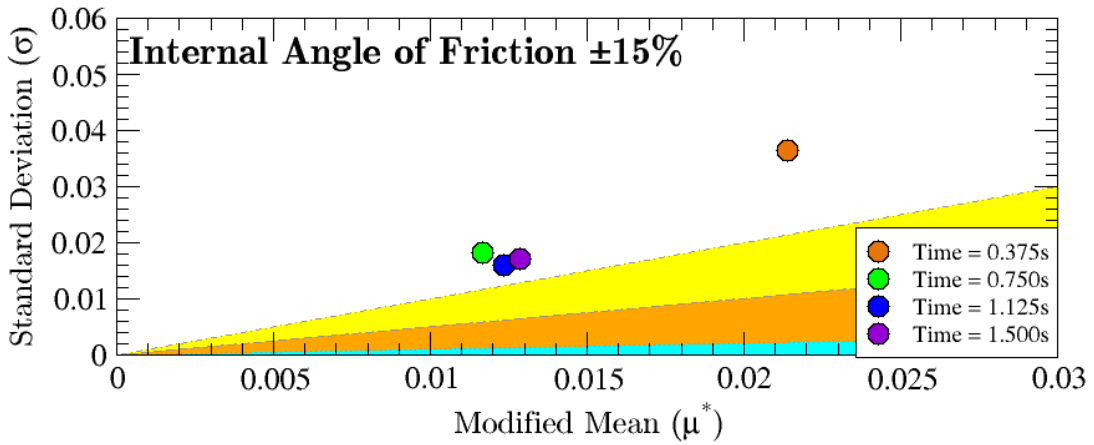

Key Points:

- All three input parameters may equally affect the mass flux and have non-linear interactions.
- No parameter is more important than the other.

Demonstration on Relevant PSI Configuration: MOAT

LaMarche - MOAT Analysis

Crater Depth

Key Points:
- Mass flow rate is strictly linear and has a (relatively) high importance.
- Internal angle of friction has a nonlinear impact at the last time stamp.
- All other points are monotonic and/or have low importance.

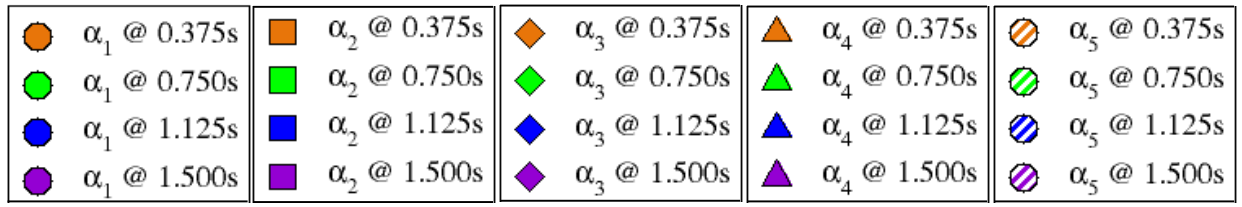

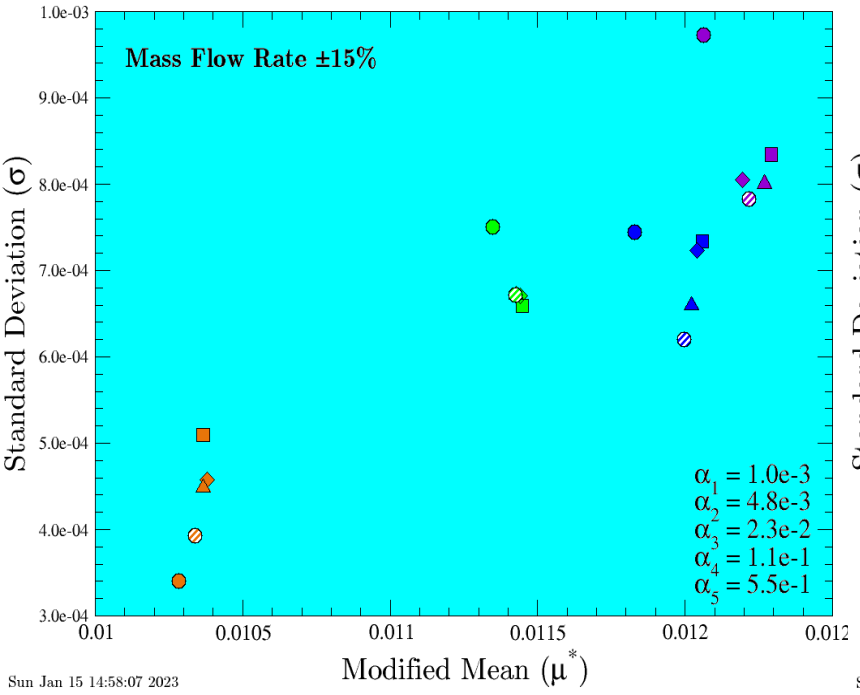

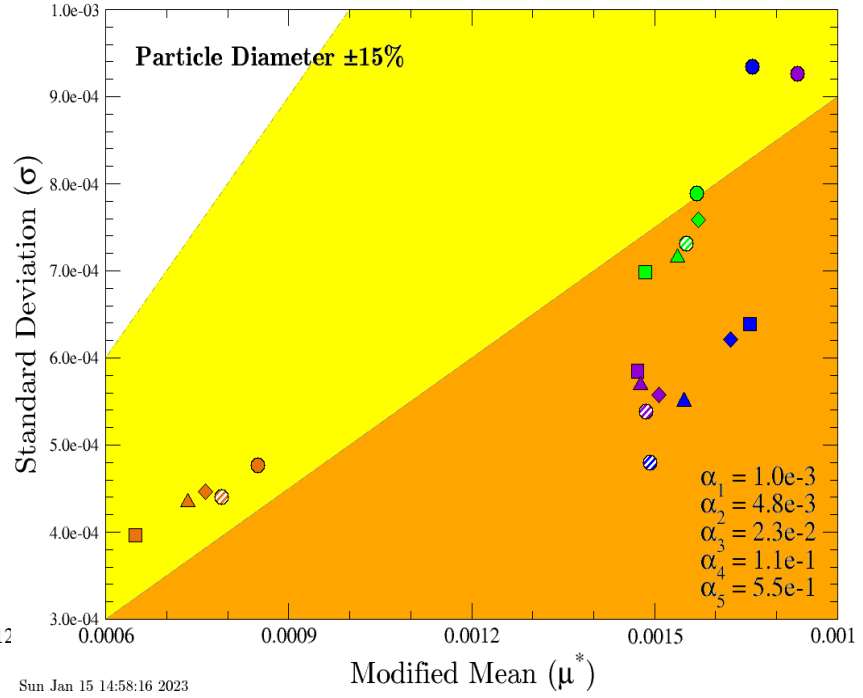

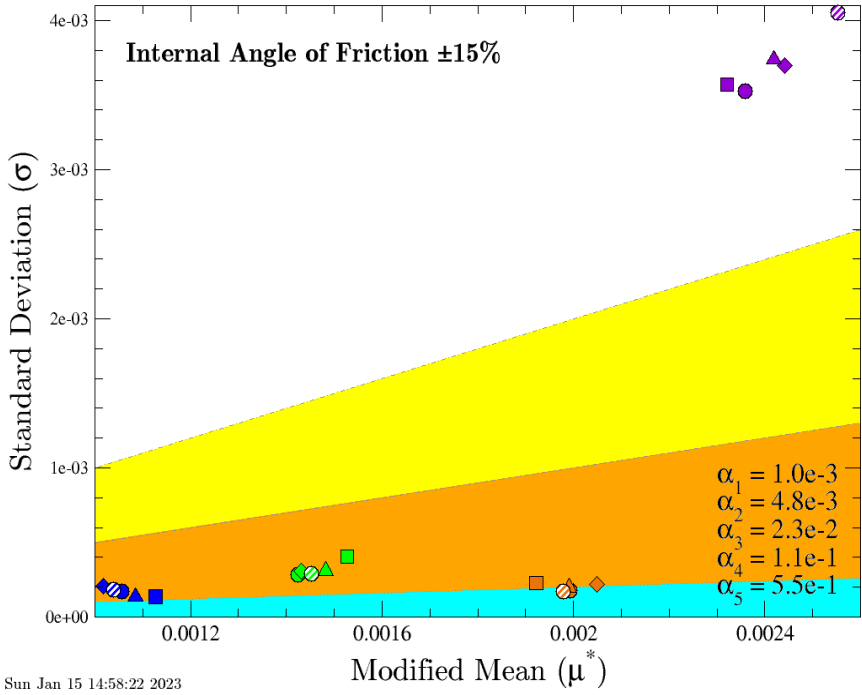

Demonstration on Relevant PSI Configuration: MOAT

LaMarche - MOAT Analysis

Crater Depth

Key Points:
- Particle diameter does not impact the depth of the crater.
- The crater depth linearly increases at each time as the mass flow of the nozzle gas increases.

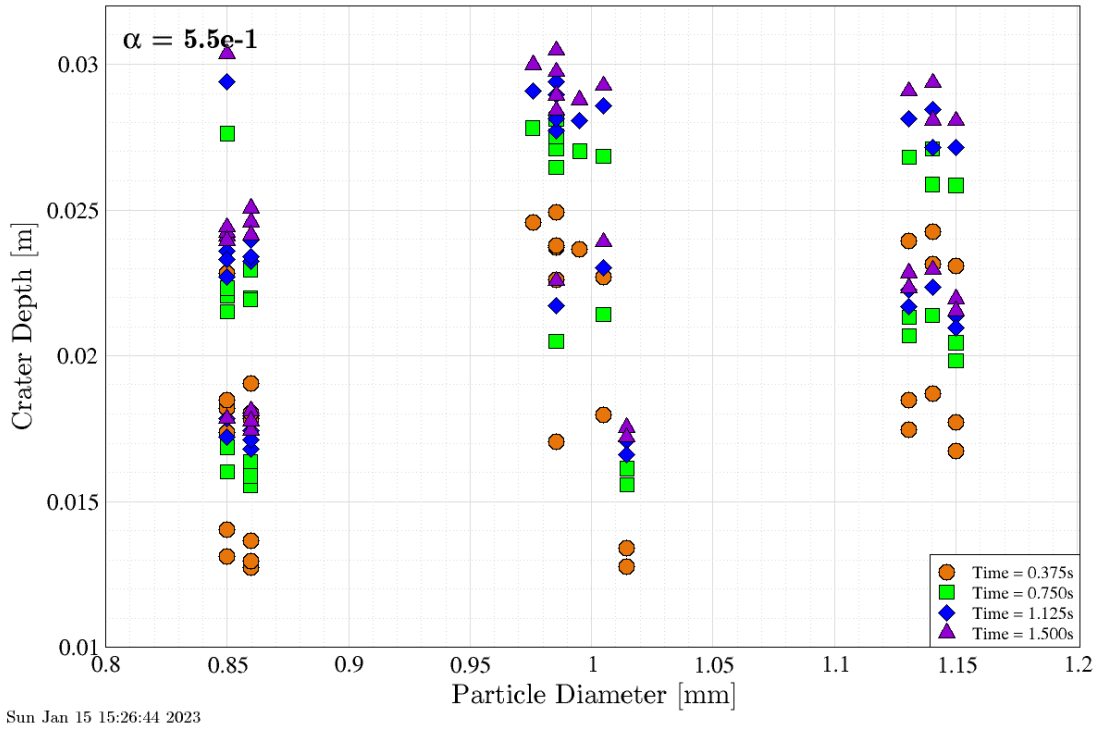

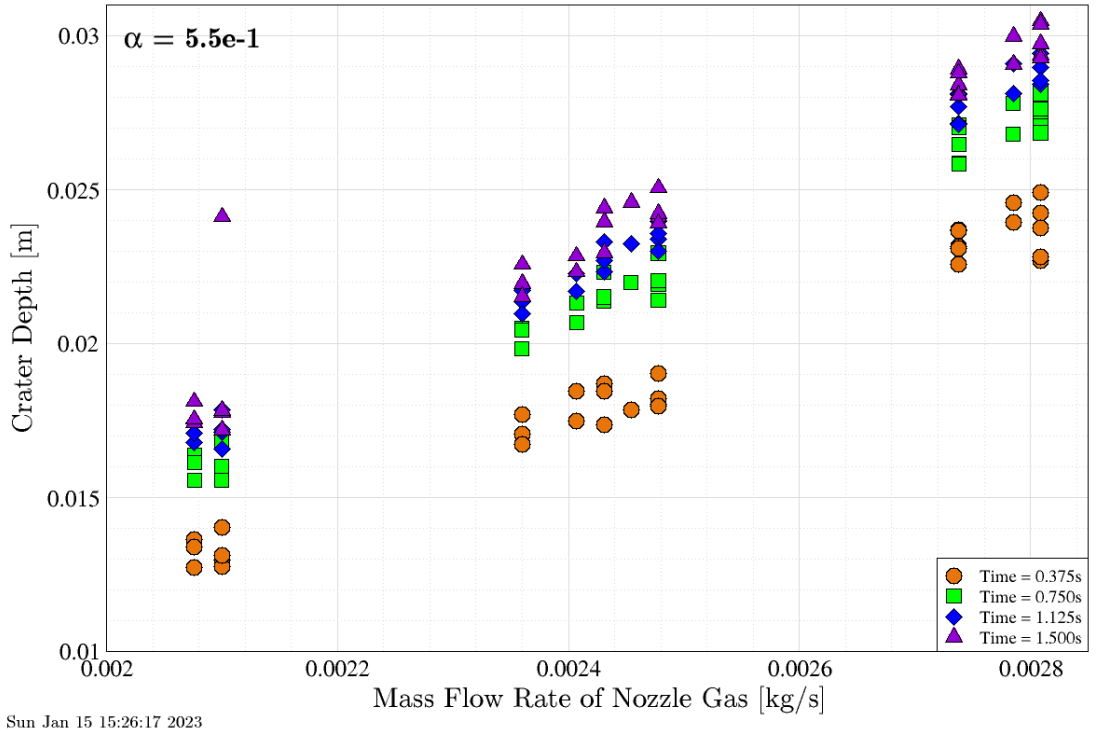

Demonstration on Relevant PSI Configuration: FAD

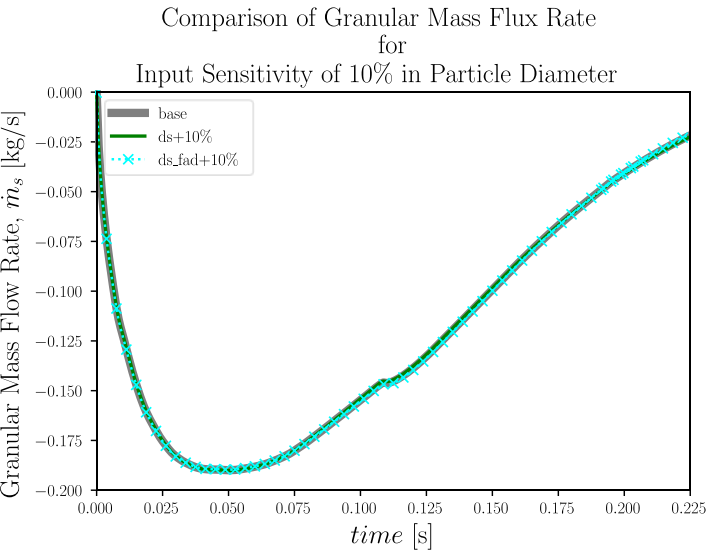

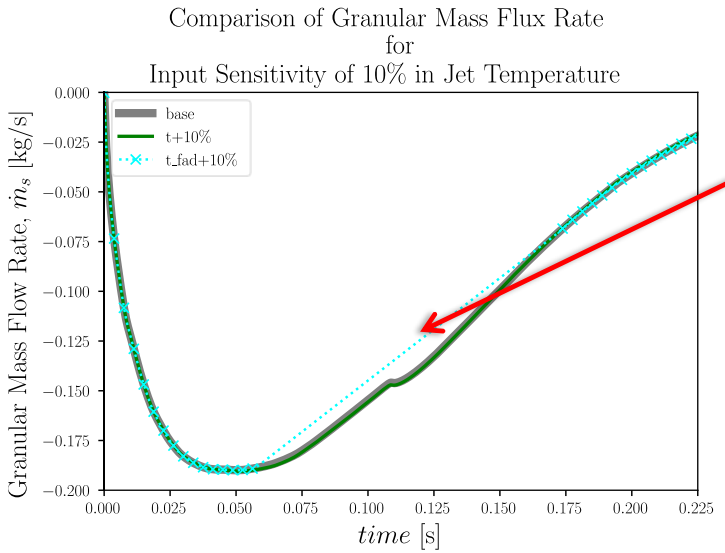

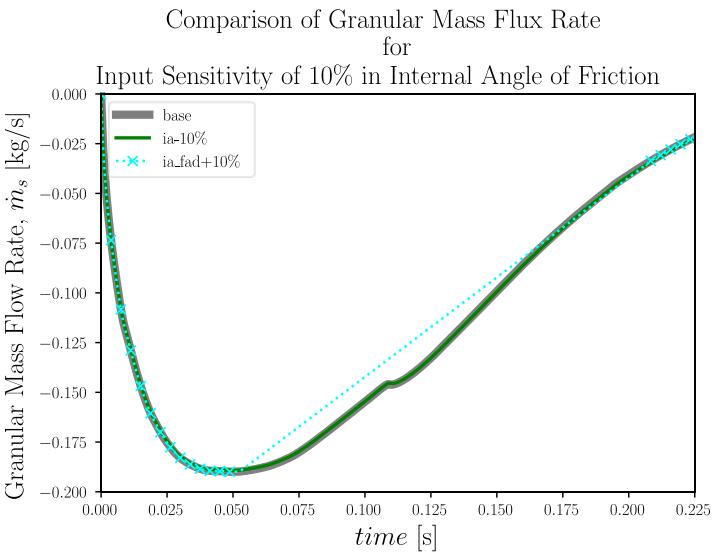

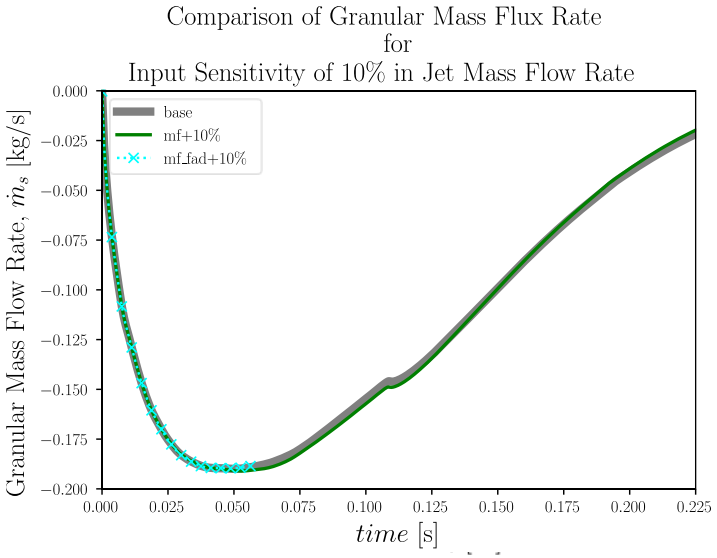

Due to PFE system issues, some data is missing in output for FAD cases.

Key Points:

- Little variation in mass excavated from crater due to any of the parameters
- FAD predicts (when data available) dynamics well

Demonstration on Relevant PSI Configuration: FAD

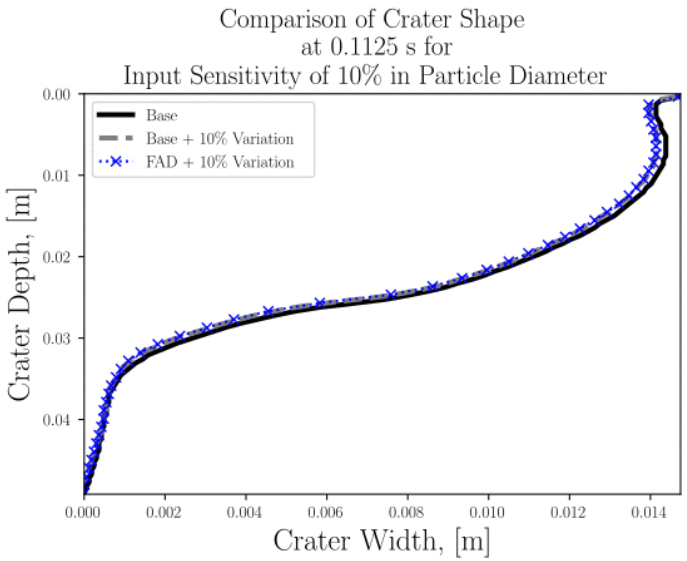

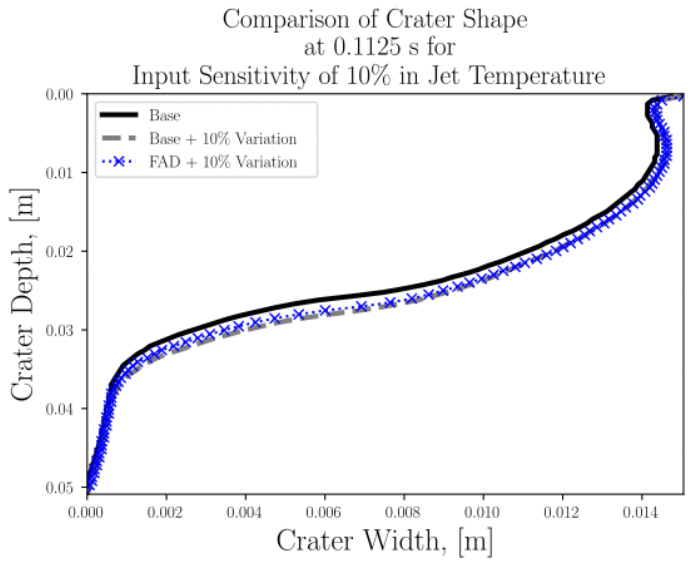

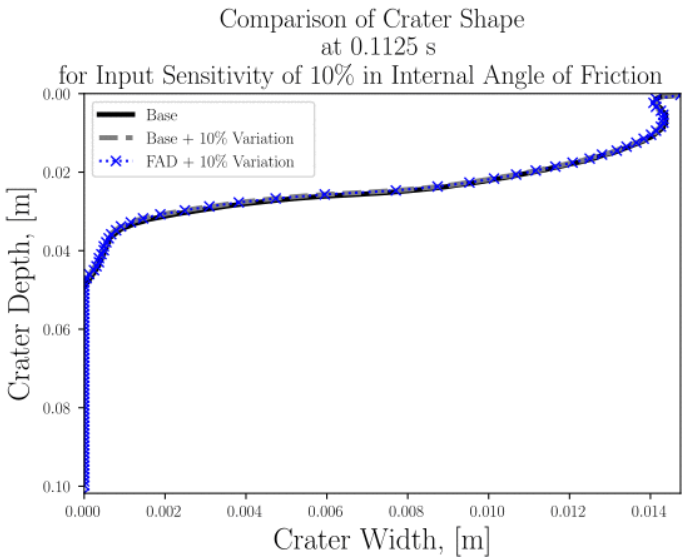

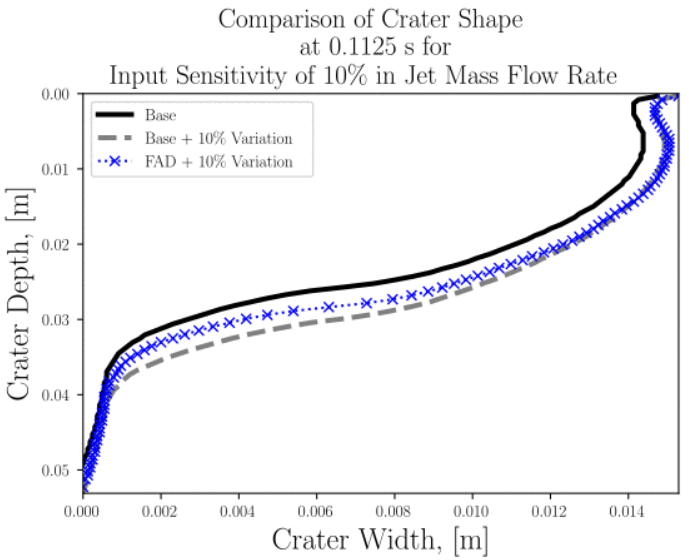

Key Points:

- Note: FAD diameter variation has issues determining depth early on due to lack of target volume fraction (0.55) in the data set
- Jet mass flow has largest effect on crater shape
- FAD predicted shape matches well with simulation data

Conclusions

- Dust was, is, and will be a major source of problems and uncertainties for any and all extraterrestrial exploration efforts
  - Using bigger rocket engines only compounds this (SEE SPACEX)
  - Landing surfaces aren't the only issue
    - Where does the dust go?
    - And why can't we see anything?
- There is no 'silver-bullet' as to which material property or model is a primary driver of uncertainty
  - We have our suspicions!
- Using sensitivity analysis, we can correctly identify sources of uncertainty within our models and approaches for PSI
  - In reality, to continue to bridge the gap between understanding and practice, a full concerted effort from both the modeling and experimental community is needed
- What's next?
  - Improve numerics to allow for second-order application of FAD (work in current Phase II)

References

- [1] Capecelatro, J., *Modeling high-speed gas-particle flows relevant to spacecraft landings: A review and perspectives.* arXiv preprint arXiv:2109.02523, 2021.
- [2] Alshibli, K.A. and A. Hasan, Strength properties of JSC-1A lunar regolith simulant. Journal of Geotechnical and Geoenvironmental Engineering, 2009. 135(5): p. 673-679.
- [3] Engelschiøn, V.S., et al., EAC-1A: A novel large-volume lunar regolith simulant. Scientific reports, 2020. 10(1): p. 1-9.
- [4] Grace, J.R., Properties, Minimum Fluidization, and Geldart Groups. Essentials of Fluidization Technology, 2020: p. 11-31.
- [5] Wang, Y., et al., On impacts of solid properties and operating conditions on the performance of gas-solid fluidization systems. Powder technology, 2007. 172(3): p. 167-176.
- [6] Seville, J., C. Willett, and P. Knight, Interparticle forces in fluidization: a review. Powder Technology, 2000. 113(3): p. 261-268.
- [7] Savage, S., *Analyses of slow high-concentration flows of granular materials.* Journal of Fluid Mechanics, 1998. **377**: p. 1-26.
- [8] Srivastava, A. and S. Sundaresan, *Analysis of a frictional–kinetic model for gas–particle flow.* Powder technology, 2003. **129**(1-3): p. 72-85.
- [9] Si, P., H. Shi, and X. Yu, *A general frictional-collisional model for dense granular flows.* Landslides, 2019. **16**(3): p. 485-496.
- [9] Francia, Victor, Lyes Ait Ali Yahia, Raffaella Ocone, and Ali Ozel. "From quasi-static to intermediate regimes in shear cell devices: theory and characterization." *KONA Powder and Particle Journal* 38 (2021): 3-25.
- [10] Al-Hashemi, H.M.B. and O.S.B. Al-Amoudi, *A review on the angle of repose of granular materials.* Powder technology, 2018. **330**: p. 397-417.
- [11] Cheng, N.-S. and K. Zhao, *Difference between static and dynamic angle of repose of uniform sediment grains.* International Journal of Sediment Research, 2017. **32**(2): p. 149-154.
- [12] Fritz, I., et al., *Repose Angles of Lunar Mare Simulants in Microgravity*
- [13] Ranjan S. Mehta, R.L.F., Manuel P. Gale, Mark Hunt, Joseph Talbot, Sami Habchi, Rui Ni, and Jesse Capecelatro, Measurement and Modeling of High Speed Polydisperse Granular Flow Under Plume/Surface Interaction Conditions. 2022, CFD Research Corporation: NASA Langley Research Center.
- [14] Capecelatro, J., Modeling high-speed gas-particle flows relevant to spacecraft landings: A review and perspectives. arXiv preprint arXiv:2109.02523, 2021.
- [15] Loth, E., et al., Supersonic and hypersonic drag coefficients for a sphere. AIAA journal, 2021. 59(8): p. 3261-3274.

Questions?